SRI International

Quarterly Technical Report #7 • February 1994

ADVANCED SEPARATION TECHNOLOGY FOR FLUE GAS CLEANUP

October-December 1993

Abhoyjit S. Bhown
Dean Alvarado
Paul Stearns
Susanna Ventura

SRI International
333 Ravenswood Avenue
Menlo Park, CA 94025

Kamalesh K. Sirkar
Sudipto Majumdar
Debabrata Bhaumick

New Jersey Institute of Technology
University Heights
Newark, NJ 07102

SRI Project No. PYU-3501

Prepared for:

U.S. DEPARTMENT OF ENERGY
Pittsburgh Energy Technology Center
P.O. Box 10940
MS 921-118
Pittsburgh, PA 15236-0940

Attn: Document Control Center

DOE Contract No. DE-AC22-92PC91344

CONTENTS

DISCLAIMER

FIGURES

TABLES

INTRODUCTION

The objective of this work is to develop a novel system for regenerable SO_2 and NO_x scrubbing of flue gas that focuses on (a) a novel method for regeneration of spent SO_2 scrubbing liquor and (b) novel chemistry for reversible absorption of NO_x. In addition, high efficiency hollow fiber contactors (HFC) are proposed as the devices for scrubbing the SO_2 and NO_x from the flue gas. The system will be designed to remove more than 95% of the SO_x and more than 75% of the NO_x from flue gases typical of pulverized coal-fired power plants at a cost that is at least 20% less than combined wet limestone scrubbing of SO_x and selective catalytic reduction of NO_x. In addition, the process will make only marketable byproducts, if any (no waste streams).

The major cost item in existing technology is capital investment. Therefore, our approach is to reduce the capital cost by using high efficiency hollow fiber devices for absorbing and desorbing the SO_2 and NO_x. We will also introduce new process chemistry to minimize traditionally well-known problems with SO_2 and NO_x absorption and desorption. For example, we will extract the SO_2 from the aqueous scrubbing liquor into an oligomer of dimethylaniline to avoid the problem of organic liquid losses in the regeneration of the organic liquid. Our novel chemistry for scrubbing NO_x will consist of water soluble phthalocyanine compounds invented by SRI and also of polymeric forms of Fe^{++} complexes similar to traditional NO_x scrubbing media described in the open literature. Our past work with the phthalocyanine compounds, used as sensors for NO and NO_2 in flue gases, shows that these compounds bind NO and NO_2 reversibly and with no interference from O_2, CO_2, SO_2, or other components of flue gas.

The final novelty of our approach is the arrangement of the absorbers in cassette (stackable) form so that the NO_x absorber can be on top of the SO_x absorber. This arrangement is possible only because of the high efficiency of the hollow fiber scrubbing devices, as indicated by our preliminary laboratory data. This cassette (stacked) arrangement makes it possible for the SO_2 and NO_x scrubbing chambers to be separate without incurring the large ducting and gas pressure drop costs necessary if a second conventional absorber vessel were used. Because we have separate scrubbers, we will have separate liquor loops and deconvolute the chemical complexity of simultaneous SO_2/NO_x scrubbing.

We will conduct our work in a 60-month period (5/92 to 4/97), encompassing 16 tasks (Table 1), beginning with studies of the fundamental chemistry and of the mass transfer characteristics of small HFC modules in the laboratory. We will then examine the most favorable method of SO_2 liquor regeneration, determine the ability of the HFC devices to withstand particulate matter,

and examine the behavior of scalable modules. In the final 15 months of the program, we will determine the fundamental mass transfer behavior of a subscale prototype system. Based on these data, a computational design model will be devised to guide further scaleup efforts that may follow.

Table 1

PROJECT TASKS AND SCHEDULE

Task Number	Title	Duration
1	Project Definition	5/92 – 6/92
2	Capacity, Reversibility and Lifetime	7/92 – 4/94
3	Chemical Synthesis	7/92 – 4/94
4	SO_2 Scrubbing with HFCs	7/92 – 2/93
5	NO_x Scrubbing with HFCs	2/93 – 10/93
6	SO_2 Liquor Regeneration	1/93 – 3/94
7	Particle Deposition	8/93 – 4/94
8	Integrated NO_x Life Tests	5/94 – 4/95
9	Scalable Modules	5/94 – 4/95
10	Computational Model	11/94 – 7/95
11	Construction of Subscale Prototype	8/95 – 1/96
12	Operation of Subscale Prototype	2/96 – 4/97
13	Refinement of Computational Model	9/96 – 4/97
14	Economic Evaluation	Various
15	Reporting	5/92 – 4/97
16	Chemical Synthesis for Process Scale-up	5/94-1/96

SUMMARY OF QUARTERLY PROGRESS

During the third quarter of 1993, we continued work on Tasks 2, 3, 4, 5, and 6. In Task 2, we tested the NO_x sorption capacity of Fe(II)-EDTA and five new SRI-synthesized compounds. We also made a comparison of all the tests so far and have selected two compounds as the leading candidates.

In Task 3, we electrochemically converted Fe(III) phthalocyanine to its Fe(II) analog and synthesized several metal phthalocyanine compounds.

In Task 4, we evaluated 200-fiber HFC modules for SO_2 removal with water and solutions of Na_2SO_3. We also connected this HFC unit to the liquor regenerating HFC unit described in Task 6. We continue to observe 95-100% SO_2 removal.

In Task 5, we calculated the overall mass transfer coefficients of earlier Fe(II)-EDTA runs for scrubbing NO_x. We also obtained a new module from Hoechst-Celanese and began its characterization.

In Task 6, we demonstrated that the spent liquor from Task 4 can be regenerated using a second HFC. The spent liquor was regenerating using DMA with initial recovery of SO_2 up to 52%.

TASK 2: CAPACITY, REVERSIBILITY, AND LIFETIME

The purpose of this task is to establish the reversible absorption capacity of the chemicals we intend to use for SO_2 liquor regeneration and for NO_x scrubbing. Any commercially successful SO_2 and NO_x chemistry must be essentially fully reversible and lose less than 10% of its activity in one year. The real issue is economics of replacement chemicals and disposal of spent chemicals. We anticipate that the maximum allowable cost for replacement and renewal of spent chemicals would be about 0.1 mil/kWh in an actual power plant operating environment.

SO_2 Absorption. To determine the reversible SO_2 absorption capacity, we have been measuring the equilibrium absorption behavior of SO_2 in an automated apparatus designed for this purpose. The apparatus measures absorption using a combination of volumetric and chromatographic techniques. We place samples of the SO_2 regeneration liquid into the sample cell and expose them to SO_2. An analysis of the SO_2 remaining after equilibrium conditions allow us to determine the absorption capacity. This experiment is repeated at various partial pressures of SO_2 that are representative of flue gas concentrations.

During last quarter, the apparatus was determined to be contaminated (see Quarterly Report #6). The first few tests in this quarter were made to ensure that the contamination problem had been corrected. These tests consisted of charging the head space and sample cell (with no absorbent present) with 10.1% SO_2 gas and allowing the system to stand for approximately 42 hours. After this period of time, the gas in the apparatus was analyzed with the Gas Chromatograph and compared to a calibration curve that had been made using the 10.1% SO_2 gas. These tests showed that the contamination problem had been solved, within the error limits of our experiments.

Since the tests performed previously (see Quarterly Report #5) on the dimer DMA (d-DMA) were not necessarily valid (it was not known whether the contamination occurred before or after the tests), four d-DMA tests were repeated. The results of these tests are shown in Table 2. In reading this table, recall that H* is defined as the volume of liquid needed to absorb an unit volume of SO_2 at STP and has the units of cm^3 liq/cm^3 (STP) SO_2.

Runs 1 and 2 were with one batch of d-DMA while Runs 3 and 4 were with another batch. Runs 1 and 2 gave the same H*, a result we did not observe in our previous set of runs (see Quarterly Report #5). In the earlier runs, we observed a decrease in sorption capacity with each run. Runs 3 and 4 are using a second batch of d-DMA and may involve leaks. These data are more suspect.

Table 2

SO_2 SORPTION BY DIMER DMA

Run #	Initial Total Pressure (Torr)	Final SO_2 Pressure (Torr)	H*, Transducer	H*, G.C.
1	764.51	4.96	0.538	0.442
2	762.81	4.853	0.552	0.442
3	953.23	3.60	0.794	0.339
4*	502.85	2.98	0.663	0.995

*There was a large leak during Run 4 which makes the data for Run 4 questionable.

Moreover, the values of H* for these tests are slightly higher than the values found in earlier tests on d-DMA. The earlier H* values were closer to 0.35 in the G. C. calculations (see Quarterly Report #5). This difference is most likely the result of contamination which made the initial capacity seem better. We now believe d-DMA may be a good candidate for SO_2 absorption and plan to continue reversibility tests with it.

After the last dimer DMA run was made, some oil from the vacuum pump leaked into the system, contaminating the lines and valves. The contaminated parts were either cleaned or reordered and the apparatus is being reassembled at this time.

NO_x Absorption. During this quarter, we completed assembly of the NO_x-absorption apparatus, whose schematic is shown in Figure 1. A mixture of NO_x/N_2 is blended with N_2 and humidified by passing it through a bubbler containing de-ionized water (Millipore Milli-Q Water Purification System) and then scrubbed by passing it through another bubbler containing a NO_x-absorbing solution. The NO_x depleted gas emerging from the second bubbler is sent to the NO_x analyzer. By monitoring the flow rates and the inlet and outlet NO_x concentrations at the bubblers over time, we can calculate the amount of NO_x absorbed by the solution. Initially, we tested our apparatus by duplicating experiments reported in the literature [E. Sada, H. Kumazawa, Y. Takada, Ind. *Eng. Chem. Fundam.*, **23**, p. 60 (1984)]. Sada et al. report the equilibrium constant K at 35°C for the reaction

$$Fe^{II}(EDTA)^{2-} + NO_e = Fe^{II}(EDTA)(NO)^{2-} \quad (1)$$

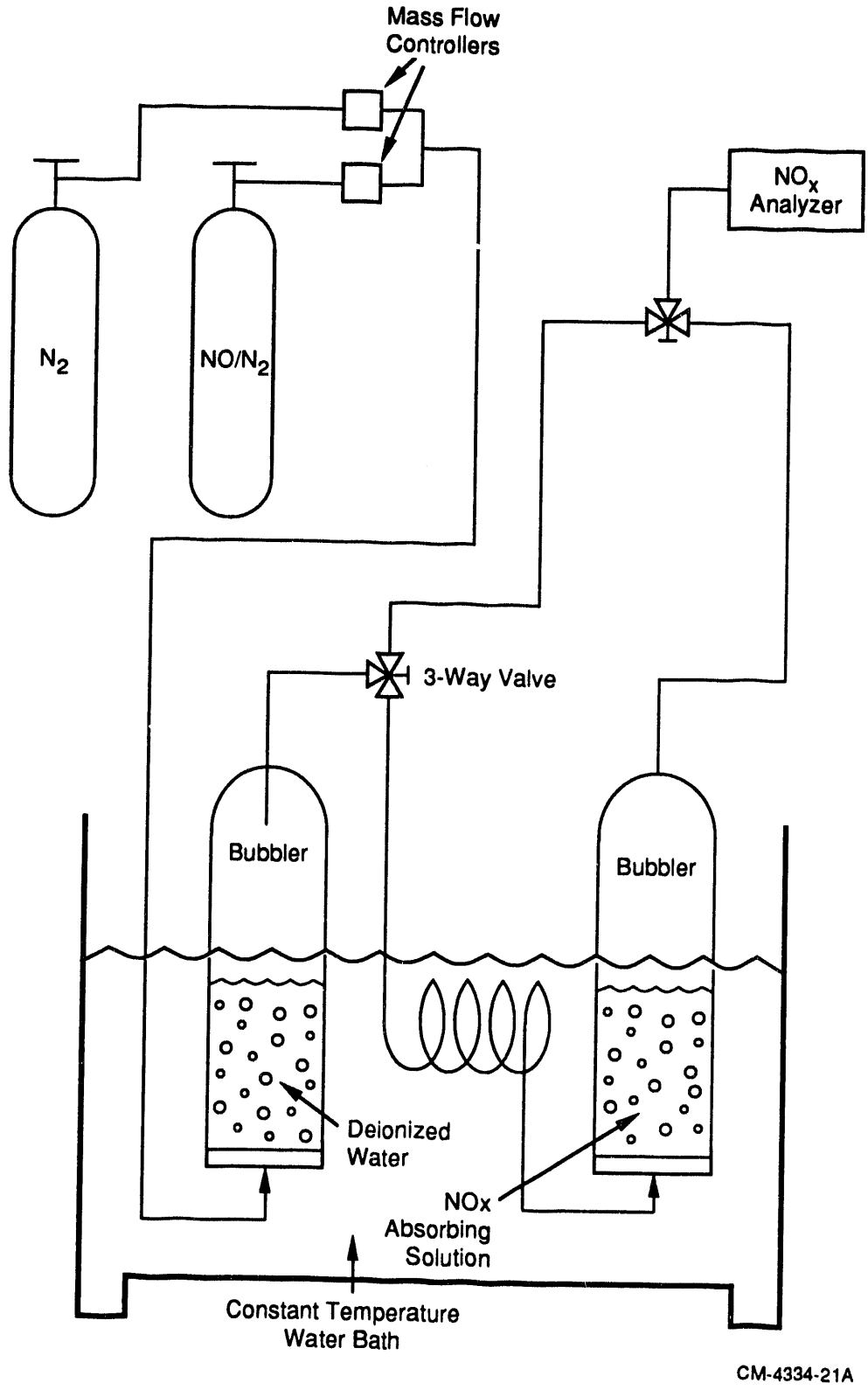

Figure 1. NO_x absorption apparatus.

concentration of NO in the liquid. Our first goal was to duplicate this result using the NO_x absorption apparatus. A 900 sccm, 990 ppm NO/Balance N_2 gas stream was used as the simulated flue gas. The NO_x-absorbing solution for this experiment was a 450 ml, 0.01 M solution of $Fe^{II}(EDTA)^{2-}$ prepared by adding equimolar amounts of ethylenediaminetetraacetic acid disodium salt-dihydrate and ferrous sulfate-heptahydrate (both from Sigma Chemical Co., St. Louis, MO). The scrubbing solution was kept at 35°C, and the gas was humidified and pre-heated to 35°C before entering the bubbler. The exiting gas stream was sent to the NO_x analyzer where its NO concentration was recorded over time. The experimental run was stopped once the exiting gas stream's NO concentration reached the inlet concentration. This experiment was performed twice to test the apparatus' reproducibility. The results of the two experiments are shown in Figure 2. This data was then used to calculate the equilibrium constant (K) for the reaction shown in Eq. (1). Details of this calculation are given in Appendix A. The values of K from both experiments were calculated to be 9.41 X 10^5 L/mol and 1.03 x 10^6 L/mol, respectively. They are close to one another, indicating reproducibility, and are within 5% of that reported by Sada *et al.*

In our next series of experiments, we performed additional NO_x-absorption runs with solutions of Fe(II)-EDTA, Fe(III)-phthalocyanine (mentioned in Quarterly Report #6), Fe(II)-phthalocyanine, Co(II)-phthalocyanine Ni-phthalocyanine and Cu-phthalocyanine-3,4',4",4"'-tetrasulfonic acid, tetrasodium salt, 85% pure (Aldrich Chemical Company, Inc., Milwaukee, Wisconsin) (Refer to Task 3 of this report for synthesis procedures). These experiments were conducted with a 0.02 M NO_x-absorbing solution, a flue gas concentration of 100 ppm NO, and a gas/liquid temperature of 25°C, similar to the NO_x scrubbing experiments with the hollow fiber contactor (Task 5). In all of the absorption runs, a 50 ml volume of a NO_x-absorbing solution was used; other conditions were similar to the two previous NO_x-absorption runs. Results from these experiments are shown in Figure 3. Note that we have plotted the axes in dimensionless quantities: C/C_0 vs. Qt/V, where C is the measured exiting NO concentration, C_0 is the inlet NO concentration, Q is the gas flow rate, t is the run time, and V is the liquid volume. As outlined in Appendix A, these results may be used to calculate the reaction equilibrium constant K of the reaction

$$M + NO = MNO \qquad (2)$$

where M represents the NO-binding compound. The results of this exercise are given in Table 3. As shown in the table, the K value for the 0.02 M Fe(II)-EDTA solution is higher than the one for the 0.01 M solution (reported above). We believe that is due to the lower temperature.

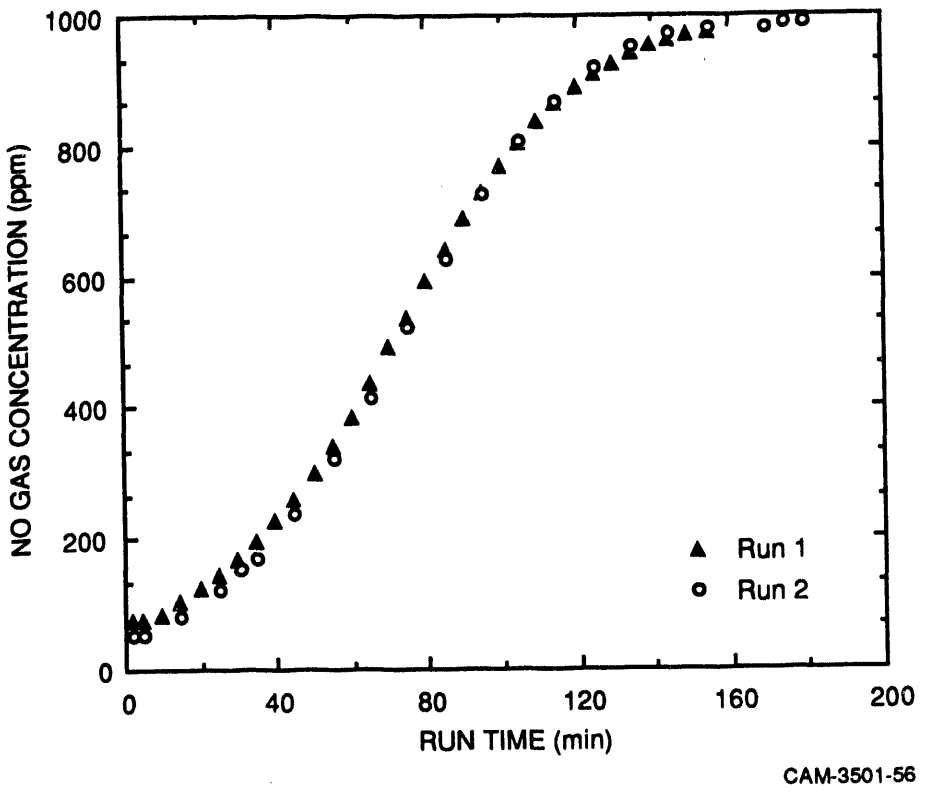

Figure 2. Exiting NO concentration versus time for the 10 mM Fe(II)-EDTA/990 ppm NO runs.

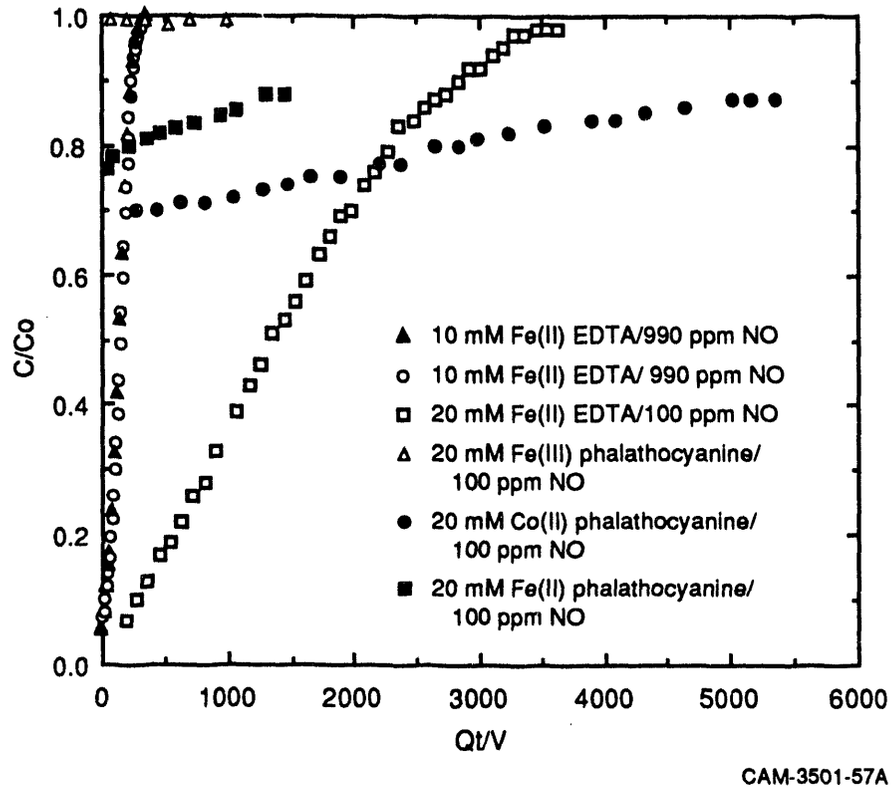

Figure 3. NO concentration over time for different scrubbing agents.

Table 3

EQUILIBRIUM CONSTANTS (K) USING 100 ppm NO IN N_2 AND 0.02 M AQUEOUS NO_X-ABSORBING SOLUTIONS AT 25°C

Compound	Equilibrium Constant, K (L/mol)
Fe(II)-EDTA	2.89×10^6
Fe(III)-phthalocyanine	0
Fe(II)-phthalocyanine	3.41×10^5
Co(II)-phthalocyanine	2.03×10^6
Ni-phthalocyanine	0
Cu-phthalocyanine	0

Also in Table 3 are the K values found for the phthalocyanine solutions. K could not be calculated for Fe(III) phthalocyanine, Ni-phthalocyanine, or Cu-phthalocyanine solutions because NO_x removal was not observed. Overall, the Fe(II)-EDTA solution is the best NO_x-absorbing compound follows by Co(II)-phthalocyanine, followed by Fe(II)-phthalocyanine. As a foot note, the Co(II)-phthalocyanine did absorb almost as much NO_x as the Fe(II)-EDTA, but it appears the kinetics to do so are much slower. However, this may not be an issue since kinetics does not usually dominate absorption in a hollow fiber contactor, mass transfer does.

Late this quarter, we repeated the experiment of determining the NO absorption capacity of Fe(II)-EDTA (described above). This was done to see if our results would be reproducible at 100 ppm NO. A 50 ml, 0.02 M Fe(II)-EDTA solution was made by mixing equimolar amounts of $FeSO_4 \cdot 7\ H_2O$ and Na_2-EDTA. As before, gas from a 1.04% NO/Balance N_2 cylinder was diluted by adding N_2 to form a 900 sccm, 100 ppm NO feed stream. The feed was sent through the NO_x-absorbing apparatus where it was heated, humidified, and contacted with the Fe(II)-EDTA solution. The temperature of the gas and of the Fe(II)-EDTA was set at 25 °C. The exiting NO concentration was monitored over time by the NO_x analyzer until it reached the feed's concentration of 100 ppm NO.

The results of this experiment are very close to those of the original Fe(II)-EDTA experiment reported last October. In Figure 4, the breakthrough curves from both experiments are similar. Also, the calculated equilibrium constants, K, for the reaction listed in Eq. (1) from both experiments agree closely. In the first experiments reported in Table 3, K was found to be 2.89 X 10^6 L/mol. In these experiment, K was calculated to be 2.7 X 10^6 L/mol. These values only

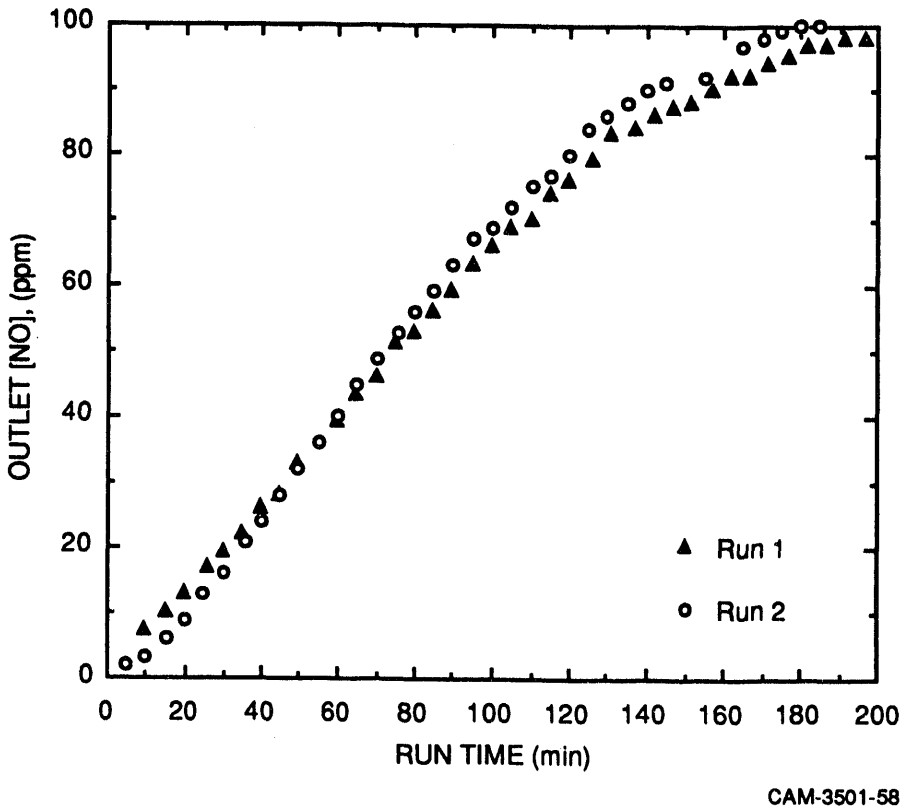

Figure 4. NOx-absorbing runs using 20 mM Fe(II)-EDTA and 100 ppm NO.

differ by 6.5%. Therefore, we have confirmed the NO absorption capacity for Fe(II)-EDTA for 990 ppm and 100 ppm NO feeds. In January, we will test a series of new NO_x-absorbing compounds. Also, we will be modifying the NO_x-absorbing apparatus to fit the characteristics of these new scrubbing compounds. The new compounds and the apparatus modifications will be discussed more thoroughly in the next monthly report.

TASK 3: CHEMICAL SYNTHESIS

The objective of this task is to synthesize oligomers of dimethylaniline (o-DMA) for our study of SO_2 liquor regeneration, and to develop compounds suitable for reversible absorption of NO_x in aqueous solutions.

NO_x Absorbents. During this quarter, we electrochemically converted the Fe(III) phthalocyanine to the correspondent Fe(II) compound. Electrolysis was performed on an aqueous solution of Fe(III) phthalocyanine (8 g in 100 mL) using a lead cathode and a Pt wire anode. The electrolysis was carried out under nitrogen using a current of 50 mA. It was not necessary to add any supporting electrolyte because of the ionic nature of the phthalocyanine compound. Therefore after reduction, no further purification was necessary and the solution was directly used for NO_x absorbing tests. The reduction of Fe(III) phthalocyanine to Fe(II) phthalocyanine was monitored by VIS spectroscopy. Figure 5 compares the VIS spectrum of Fe(II) and Fe(III) phthalocyanine. Additionally, we prepared the tetrasodium salt of Ni(II) 4,4',4",4"'-tetrasulfophthalocyanine.

Nitric oxide is known to form a coordination complex with Fe^{2+}-EDTA whose reaction rates are very fast. The drawback of this chemistry is that the regeneration process has proven to be quite expensive because the Fe^{2+} species is oxidized readily to the ineffective Fe^{3+} species.

To overcome the limitations of the Fe^{2+} -EDTA NO_x removal process, we are developing polymeric analogs to EDTA. This approach is conducted in parallel to the development of phthalocyanine based sorbents. While to date no information has been reported on the lifetime of polymeric analogs to EDTA, we can expect that their lifetime will vary with the nature of the polymer backbone and the reversible adsorption capacity for NO will vary with structural changes.

Also during this quarter, we worked on the synthesis of polymeric analogs to EDTA. To be of practical use, these polymers should be soluble in water. Accordingly, we have initially focused our efforts on the functionalization of polyethyleneimine, a water soluble polymer. In one approach, we functionalized poly(ethyleneimine) by alkylation with chloroacetic acid. The resulting polymer was found to be soluble in water. However, upon addition of Fe^{2+} a crosslinked gel was formed. We believe that gelation is taking place because of the intermolecular formation of the Fe^{2+} complex. To minimize intermolecular complexation and instead favor the intramolecular process, it is desirable to functionalize the polymer with iminodiacetic acid. Accordingly, we have attempted to functionalize polyethyleneimine with ethylenediaminotetracetic dianhydride. The resulting polymer is however partially crosslinked.

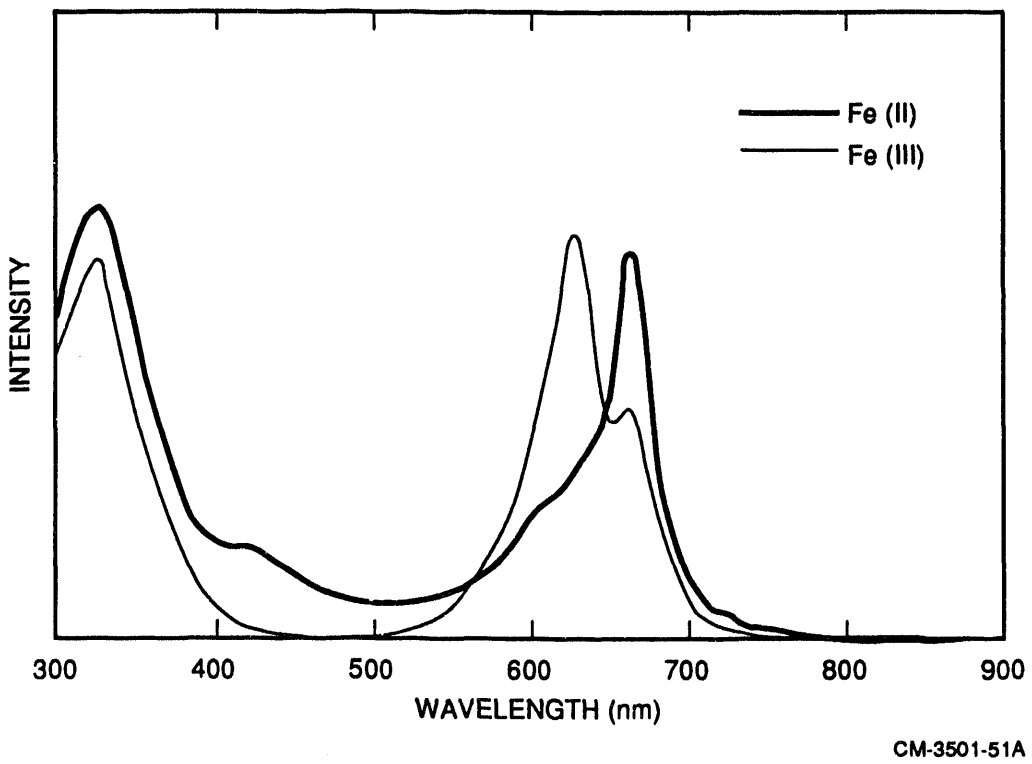

Figure 5. UV-visible spectrum of tetrasodium salt of iron 4,4',4",4"' tetrasulfophthalocyanine.

We are currently developing a polymeric analog to EDTA by functionalization of poly(allylamine) with chloroacetic acid. We expect that this polymer will allow us to overcome the limitations of the previously synthesized polymers. The polymer is expected to be mainly bind Fe^{2+} intramolecularly and is not expected to crosslink during reaction.

TASK 4: SO_2 SCRUBBING WITH HOLLOW FIBER CONTACTORS

The objective of this task is to determine the mass transfer characteristics of hollow fiber contactors (HFCs) for scrubbing SO_2 from a simulated flue gas. These devices have been shown to remove more than 99% of the SO_2 from a simulated flue gas. However, mass transfer principles in HFCs are not established on a sound basis, especially for a system with a liquid phase chemical reaction.

Under subcontract to SRI, Dr. K. Sirkar at the New Jersey Institute of Technology (NJIT) is responsible for Task 4. In this task, we intend to gather a series of steady mass transport data under various conditions. We will systematically vary the gas flow rate, the liquid flow rate, the liquid composition, and the HFC module properties. We will perform experiments both at room temperature and at 70°C. This work will be dc _ with small modules in cylindrical form to achieve a well-defined flow distribution in the module.

During this quarter, we completed one absorption-only run and six simultaneous absorption runs of SO_2 by an aqueous solution of Na_2SO_3 and regeneration of the spent liquor by extraction with dimethylaniline (DMA). Details on the absorption part of these runs are presented in this section.

The sulfite liquor was pumped through the shell side of the 200-fiber module. The first three runs, AE-4 to AE-6, used a model flue gas with an initial composition of 2300 ppm of SO_2, 2.9% O_2, 10.5% CO_2 and balance N_2. The second three runs, AE-7 to AE-9, used a model flue gas with an initial composition of 2170 ppm of SO_2, 3.13% O_2, 3.13% O_2, 10.8% CO_2 and balance N_2. The residual composition of SO_2 at the outlet of this module was measured by sampling the treated flue gas in a GC. A steady state condition for the absorption process was reached after about 5-6 hours. The effluent sulfite solution was then fed into the tube side of the 1000-fiber module and liquid DMA was pumped through the shell side of this extractor unit. The SO_2 concentration in DMA at the exit was determined by wet chemistry, from which its flux at the extraction stage was calculated. The corresponding SO_2 flux from the flue gas to the aqueous phase in the absorption step was obtained from material balance. The run-parameters and the absorptive fluxes are presented in Table 4.

In Run AE 4, the flue gas was humidified before being fed into the module. Dry gas from the cylinder was utilized in Runs AE 5 and 6. The flow rate of the sulfite liquor was changed to 10 ml/min in Run AE 6 to examine its effect on the extraction process. We monitored the pH of both the aqueous effluent from the absorption unit and that from the extraction unit. An increase in the pH of the stream after extraction was anticipated since SO_2 was removed at this step. We did not observe any significant change (see Table 4).

Table 4

SUMMARY OF ABSORPTION DATA IN SIMULTANEOUS ABSORPTION-EXTRACTION RUNS

Run No.	Aqueous Absorbent Type	Aqueous Absorbent Flow Rate mL/min	Flue Gas Flow Rate sccm	Flue Gas SO_2 Composition ppm Inlet	Flue Gas SO_2 Composition ppm Outlet	Absorptive Flux of SO_2 moles/cm^2 sec	Steady State pH of Aqueous Stream, After Absorption	Steady State pH of Aqueous Stream, After Extraction
AE-4*	0.2 M Na_2SO_3	20	2722 (Humidified)	2250	69	1.02×10^{-8}	7.35	7.4
AE-5*	0.2 M Na_2SO_3	20	2704 (Dry)	2300	43	1.05×10^{-8}	7.7	7.8
AE-6**	0.2 M Na_2SO_3	10	2732 (Dry)	2300	100	1.038×10^{-8}	7.3	7.3
AE-7*	0.2 M Na_2SO_3	20	2732	2170	44	0.996E-08	7.55	7.75
AE-8*	0.2 M Na_2SO_3	20	2732	2170	60	0.990E-08	7.4	7.5
AE-9***	0.2 M Na_2SO_3	30	5000	2170	142	1.721E-08	7.3	7.65

* DMA flow rates were different at the extraction stage.
** The liquid flow rate at the absorption part was decreased.
*** Both the gas and liquid flow rates at the absorption part were increased.

Dry gas from the cylinder was used in Runs AE 7, 8, and 9. The flow rate of the DMA was varied at the extraction stage; otherwise the absorption segment of Runs 7 and 8 were similar to that of Runs AE 5 and 6. In Run AE 9, the flow rate of the sulfite liquor was increased to 30 ml/min to examine its effect in reducing the boundary layer resistance at the downstream extraction process. The gas flow rate was increased to 5 slpm to adapt to the increased liquid flow rate and help attain low residual concentration of SO_2 at the outlet of the absorption unit. After about 3 hours, the SO_2 level in the treated flue gas reached a value of 144 ± 5 ppm. It remained there for the rest of the runtime of 4 hours that included the extraction process. It was the highest gas flow rate we ever employed. A steady absorption process was in effect with an increased flow of aqueous sulfite liquor. The high flow rate of the liquid allowed the operation without any pore drying though the incoming flue gas was no' humidified. We monitored the pH of both the aqueous effluents from the absorption unit and that from the extraction unit. A minor increase in the pH of the stream after extraction was observed in these three runs. See Table 4.

In continuing our efforts to obtain a situation where the resistance to mass transfer shifts to the gas phase, two absorption-only experiments were conducted this quarter. The first, A-17, was run with the flow rate of the humidified incoming flue gas set at approximately 3630 sccm and other conditions were identical to those absorption-only runs reported previously. The model flue gas had an initial composition of 2300 ppm SO_2, 2.9% O_2, 10.5% CO_2 and balance N_2. The results are presented in Table 5, which also includes results of absorption part of the above extraction-absorption runs with the sulfite solution.

The second absorption-only experiment conducted this quarter is numbered A-18. The model flue gas had an initial composition of 2170 ppm SO_2, 3.13% O_2, 10.8% CO_2 and balance N_2. It was humidified before being fed into the module. The flow rate of this incoming flue gas was 4500 sccm. Increase of the gas flow rate was in line with the experimental pattern we adopted in recently completed absorption-only runs when other conditions were identical. The incoming flue gas was humidified by passing it through the tube side of two HFC modules whose shell sides were filled with water maintained at 10 psig. The high gas flow rate of 4500 sccm introduced a larger amount of moisture in the stream. It was difficult to remove this moisture completely from the sample effluent going into the GC by the Nafion membrane drier. After 3 hours, the effluent compositions of SO_2, other components and water vapor attained a constant level. The SO_2 composition was 148 ± 8 ppm with repetitive fluctuations showing a steady state run-condition. The results are presented in Table 5, which includes results of absorption part of the above extraction-absorption runs.

Table 5

RESULTS OF SO_2 ABSORPTION RUNS USING 0.2 M Na_2SO_3 AT 20 mL/min

Run No.*	Temp. °C	Liquid Flow Rate mL/min	Gas Flow Rate sccm	SO_2 Composition, ppm Inlet Dry	Inlet Humid	Outlet	SO_2 Removal (%)	K_g cm/s
AE-4	19	20	2732	2300	2250	69	97	0.345
AE-5	22	20	2704	2300		43	98	0.395
AE-6	19	10	2723	2300		80	97	0.332
A-17	20	20	3630	2300	2243	100	96	0.397
AE-7	19	20	2732	2170		44	98	0.384
AE-8	19	20	2732	2170		60	97	0.354
AE-9	19	30	5000	2170		142	93	0.465
A-18	18.5	20	4500	2170	2150	148	93	0.416
A-15	22	20	2704	2400	2243	67	97	0.345
A-12	28	20	2713	2210	2050	65	97	0.349

*AE - indicates Absorption-Extraction run.

A - for Absorption-only run.

The steady state condition for the absorption process was achieved in many runs employing a flow rate of 20 ml/min for the aqueous-sulfite-solution and gas flow rates varying between 1800-4500 sccm. Majority of the runs employed liquid and gas flow rates as 20 ml/min and about 2700 sccm respectively, a combination often used in absorption-extraction runs. Typical values of the mass transfer coefficient obtained from some of these runs are plotted in Figure 6 against the corresponding gas flow rates. Sample values are from Table 5. The plot shows a pattern in which K_g increases with the gas flowrate, and that dependency becomes smaller at higher gas flowrates. The data trend is toward gas-phase controlled mass transfer.

Previously, an analysis of results of some flue-gas-absorption experiments with 0.2 M Na_2SO_3 was reported. We compared the conversions of SO_2 and CO_2 that occurred simultaneously. The analysis suggested that the reaction between SO_2 and aqueous Na_2SO_3 can be considered instantaneous. Typically, a ratio of about 4:1 was maintained between the amount reacted for SO_2 and CO_2. The depletion of CO_2 was less significant with respect to that of SO_2.

A separate run was also conducted using 0.2 M Na_2SO_3 to absorb a gas mixture of CO_2-N_2 containing 9.89 % CO_2. A model flue gas usually consists of about 2500 ppm SO_2, 10% CO_2, 3% O_2 and balance N_2. The purpose in this experiment was to gather data on the extent of reaction that could occur between CO_2 and the sulfite liquor in the 200-fiber contactor in the absence of SO_2 and O_2. The gas flow rate was about 2700 sccm and the liquid flow rate was 20 mL/min, similar to those of a typical run in absorbing flue gas. A steady state condition was obtained after about two hours, and the run continued for an additional hour. An estimation of GC results indicated that 4.34% of the incoming CO_2 reacted with the sulfite solution. It amounted to a removal of 4290 ppm from 98,900 ppm of inlet CO_2. In the case of flue gas absorption, the SO_2 composition dropped typically from about 2300 to 50-80 ppm. The amount of CO_2 consumed in a parallel reaction was estimated to be approximately 500 ppm. The selectivity of reactions with sulfite is favored for SO_2. We plan to continue to examine the speed of the reactions of SO_2 and CO_2 with the sulfite solution.

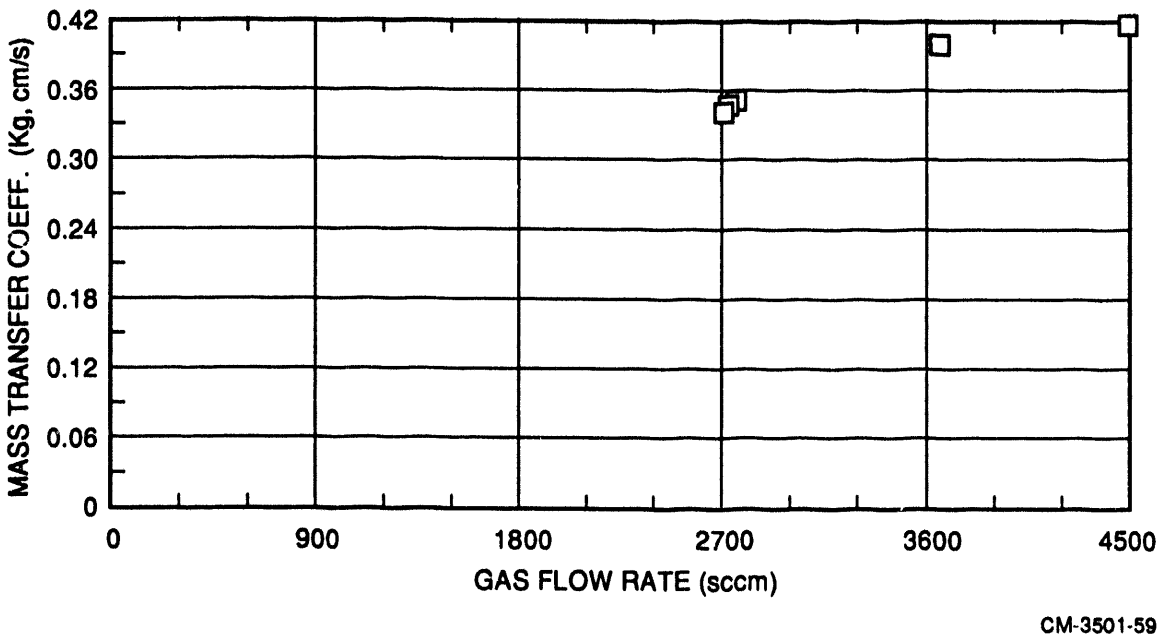

Figure 6. Variation of mass transfer coefficient with gas flow rates at an aqueous sulfite solution flow of 20 ml/min.

TASK 5: MASS TRANSFER RATE STUDIES FOR NO_X SCRUBBING IN HOLLOW FIBER CONTACTORS

The objective of this task is to determine the mass transfer characteristics of hollow fiber contactors (HFCs) for scrubbing NO_x from a simulated flue gas. NO and N_2 are blended at controlled rates, passed through a humidifier, checked for composition, heated, and fed into the lumens of the hollow fibers. The scrubbing liquid is pumped at a controlled flow rate, filtered, heated, and fed into the shell-side of the hollow fiber module. Pressure and temperature probes at various locations allow us to monitor and control the experimental conditions.

During this quarter, we calculated the overall liquid-side mass transfer coefficients (K_{olm}) for the 301 fiber HFC. This was done by using the experimental results from the NO_x-absorption runs (Task 2). After determining the equilibrium constant (K) for the 100 ppm NO/20 mM Fe(II)-EDTA run, we calculated and plotted the total concentration of NO absorbed in the liquid solution as a function of the NO concentration in the gas. At the lower gas phase concentrations of NO, the curve is fairly linear. As a result, the partition coefficient (H) for a 20 mM Fe(II)-EDTA solution was estimated to be the slope of the curve at the lower NO gas phase concentrations. The slope would equal H, and this was calculated to be 6.961×10^{-5} mol/L-atm. With H, we determined the K_{olm} for the 301 fiber HFC. This calculation was performed using the data from the HFC experiments where 80-85% NO removal was observed (see Quarterly Report #6). In the experiment with 20 mM Fe(II)-EDTA and a gas flow rate of 290 sccm, about 80% of the NO was scrubbed from the flue gas. K_{olm} calculated for this experiment is 7.15×10^{-6} cm/sec. Also, for the experiment with a 200 sccm gas flow rate, more than 85% NO removal was achieved. K_{olm} for this experiment was calculated to be 7.51×10^{-6} cm/sec. Since these values of K_{olm} are much lower than that obtained using CO_2, we plan to continue characterizing the 301 fiber HFC with Fe(II)-EDTA as the scrubbing solution. One possibility is that there may be pore condensation between runs or perhaps deposition of Fe(II)-EDTA crystals onto pores during a run.

Also this quarter, we received a new 1000 fiber HFC from Hoechst-Celanese. The fiber openings on both ends of this HFC look better than our original one. However, we found that Hoechst-Celanese sent us a module with a baffle at its center. Our previous 1000 fiber HFC did not have this baffle. Therefore, Hoechst-Celanese volunteered to make us a new HFC without a baffle. We received the new module, photographed the module ends, and counted 1169 fibers.

TASK 6: SO_2 LIQUOR REGENERATION

The objective of this task is to determine the fundamental mass transfer characteristics of hollow fiber contactors for regenerating aqueous SO_2 scrubbing liquor with organic solvents having a high affinity for SO_2. So far we have reported results on absorption of SO_2 by an aqueous solution of 0.2 M Na_2SO_3 solution and deionized water and subsequent regeneration of the spent liquor by extraction with dimethylaniline (DMA). We have carried out further test runs on simultaneous absorption and extraction with an aqueous solution of 0.2 M Na_2SO_3 solution as an absorbing liquid and DMA as an organic extractant. In these runs we have studied the effect of aqueous and organic flow rates on the SO_2 recovery by the extraction process.

In the last quarterly report we mentioned that we modified the setup by installing three additional valves in the aqueous line in order to allow the aqueous stream to bypass the second module (extraction) altogether when we run our experiment only in absorption mode. The modified combined absorption/extraction setup is shown in Figure 7. A certified gas mixture consisting of 2300 ppm SO_2, 10.5% CO_2, 2.9% O_2 and balance N_2 was sent through the tube-side of module containing 200 hollow fibers (fiber ID and OD: 240 and 300 microns, respectively). An aqueous solution of 0.2 M Na_2SO_3 was passed through the shell-side. The exit aqueous stream was introduced to the tube-side of the second crossflow hollow fiber module containing 1000 fibers (fiber ID and OD: 240 and 300 microns, respectively) only when a steady state in the absorption apparatus was achieved. In all runs a constant model feed flue gas flow rate of ~2700 sccm was maintained. In the first run (no: AE 4, Table 5), the feed gas was humidified but in the other two cases, the model flue gas was introduced without humidification.

Three runs were done, AE-4, 5, and 6. In runs AE 4 and AE 5 (Table 5), the flow rate of the aqueous solution was kept at 20 ml/min but the organic flow rate was changed from 6.9 to 4 ml/min. At higher organic flow rate the SO_2 concentration in DMA was lower but the total SO_2 transfer was higher. Comparing runs AE 4 and 6, we see that the SO_2 transfer rate decreased by about 50% when the aqueous flow rate was changed from 20 ml/min to 10 ml/min. The summary of extraction data and the flux of SO_2 during regeneration are shown in Table 6. In these runs only a maximum of 13% of the absorbed SO_2 was recovered by the organic liquid. Note that in our earlier runs with water (see last progress report), we have obtained much higher recoveries. Therefore, further experiments will be carried out at higher flow rates.

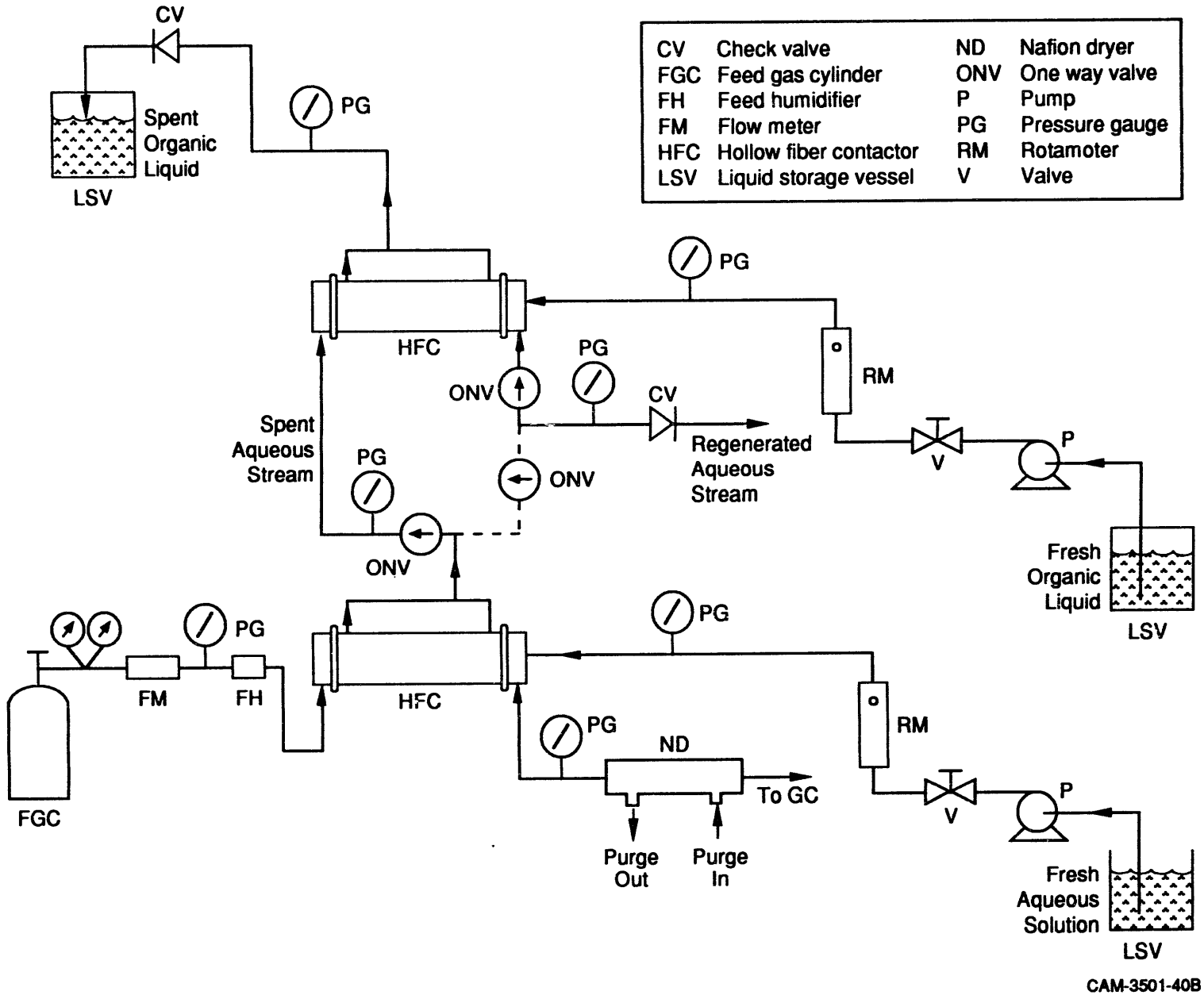

Figure 7. Schematic of combined absorption and liquor regeneration setup.

Table 6

SUMMARY OF EXTRACTION DATA IN SIMULTANEOUS ABSORPTION-EXTRACTION RUNS

Run No.	Aqueous Absorbent Type	Aqueous Absorbent Flow Rate mL/min	Flue Gas Flow Rate sccm	Flow Rate of DMA mL/min	SO_2 Concentration in DMA mole/cc	Extractive Flux of SO_2 moles/cm^2 sec	SO_2 Transfer Moles/sec. at Absorption	SO_2 Transfer Moles/sec. at Extraction	Percent Recovery by Extraction
AE-6	0.2 M Na_2SO_3	10	2723 (Dry)	6.1	2.93E-06	1.72E-10	4.50E-06	2.98E-07	6.6
AE-4	0.2 M Na_2SO_3	20	2732 (Humidified)	6.9	4.97E-06	3.30E-10	4.43E-06	5.72E-07	13.0
AE-9	0.2 M Na_2SO_3	30	5000 (Dry)	6.4	6.21E-06	3.82E-10	7.46E-06	6.62E-07	8.9
AE-5	0.2 M Na_2SO_3	20	2704 (Dry)	4.05	6.68E-06	2.60E-10	4.54E-06	4.51E-07	9.9
AE-4	0.2 M Na_2SO_3	20	2732 (Humidified)	6.9	4.97E-06	3.30E-10	4.43E-06	5.72E-07	13.0
AE-7	0.2 M Na_2SO_3	20	2723 (Dry)	16	2.67E-06	4.11E-10	4.32E-06	7.12E-07	16.5
AE-8	0.2 M Na_2SO_3	20	2732 (Dry)	31	3.31E-06	9.75E-10	4.29E-06	1.69E-06	39.4
AE-10	0.2 M Na_2SO_3	10	2459 (Dry)	38	3.33E-10	12.17E-10	4.01E-06	2.11E-06	52.6

For regenerating aqueous SO_2 scrubbing liquor, two alternative processes were suggested in the research proposal: liquid-liquid extraction (LLE) and extraction via hollow fiber contained liquid membrane (HFCLM) technique. In the second technique, dimethylaniline will be utilized as a membrane in a contained liquid membrane device containing two different sets of fibers. The HFCLM module required in this project is made of two different kinds of fibers. One set of fibers would be microporous hollow fibers (e.g., Celgard) and the other set would be made of nonporous material such as silicone. We will fabricate such a module in our laboratory. We are currently taking decisions about the fibers to be used in such a module.

Next, to study the effect of organic and aqueous flow rates on the SO_2 transfer in the extraction process, we carried out additional test runs on simultaneous absorption and extraction with an aqueous solution of 0.2 M Na_2SO_3 solution as an absorbing liquid and DMA as an organic extractant. In membrane solvent extraction, the overall resistance to solute transfer comes from three resistances in series: the aqueous and organic film resistances and the membrane resistance. By increasing the fluid flow rates, the aqueous and organic resistances could be reduced and an improvement in mass transfer would result.

In the next set of experiments the gas mixture used as a feed to the absorption module had a composition of 2170 ppm SO_2, 3.13% O_2, 10.8% CO_2 and balance N_2. These runs are numbered AE-7, 8, and 9. The aqueous and organic flow rates were varied systematically in the combined setup and the SO_2 concentration in the DMA was determined in a manner described in our earlier reports. The results are also reported in Table 6. The effect of aqueous absorbent flow rate variation is presented in the first part of the table whereas that of organic flow rate variation is presented in the second part. In all runs except run AE 9, a constant feed flue gas flow rate of ~2700 sccm was maintained. We see an increase in SO_2 transfer in the extraction process (by a factor of 2.2) as the absorbent flow rate was increased from 10 to 30 ml/min, keeping the organic flow rate constant at ~6 ml/min. Note that the run AE 9 was carried out at a different condition where the gas flow rate to the absorption module was 5000 sccm. A very high gas flow rate was used in order to obtain a reasonable amount of SO_2 at the exit gas stream. It was anticipated that all of the SO_2 present would be absorbed at the lower gas flow rate of ~2700 sccm and aqueous Na_2SO_3 solution flow rate of 30 ml/min. A higher organic flow rate under these conditions would result in a higher percent recovery in the extraction process.

In the second part of the table, we have presented the data obtained by varying the organic flow rate. In all these runs the feed gas and the aqueous solution flow rates were maintained at constant values. It is clear that the SO_2 transfer in the extraction process increased substantially as the organic flow rate was increased from 4 to 31 ml/min. We were able to recover about 40% of the

absorbed SO_2 from the aqueous solution when the organic liquid flow rate was 31 ml/min. It is possible to recover even more of the absorbed SO_2 by manipulating the aqueous and organic flow rates and by providing a larger contact area.

Finally, we conducted an additional run this quarter, AE-10. A certified gas mixture consisting of 2230 ppm SO_2, 11% CO_2, 3.20% O_2 and balance N_2 was passed through the tube-side of module containing 200 hollow fibers without humidification. The flue gas flow rate was about -2450 scc/min. An aqueous solution of 0.2 M Na_2SO_3 was passed through the shell-side. The exit aqueous stream was allowed to bypass the extraction module during the time period needed to achieve a steady state in the absorption apparatus. Once a steady outlet gas composition was achieved, the extraction part of the experiment was initiated with DMA flow in the shell side and by introducing the exit aqueous stream to the tube-side of the second crossflow hollow fiber module containing 1000 fibers. Normally, it takes 3 to 5 hrs to achieve a steady state in the absorption part of the experiment. However, out of three trial runs, we were able to achieve a steady state in only one. Two runs were abandoned when we did not get a constant outlet SO_2 composition in more than a 6-hour period.

In our earlier experimental results, we have seen that the SO_2 transfer in the extraction increases substantially with increase in organic flow rate. Therefore, in run AE-10, the organic flow rate was kept at a high value of 38 mL/min whereas the aqueous flow rate was maintained at 10 mL/min as shown in Table 6. Under these conditions, it was possible to recover more than 50% of the absorbed SO_2 from the loaded aqueous 0.2 M Na_2SO_3 solution. Note that as the organic flow rate is increased from ~4 mL/min to 38 mL/min (9.4 times), the extractive flux of SO_2 increased from 2.60×10^{-10} to 12.17×10^{-10} moles/cm^{2}sec (4.7 times). The total SO_2 transfer also increased from a value of 4.51×10^{-7} to 2.11×10^{-6} moles/sec. Further increase in SO_2 recovery is possible with even higher organic flow rate. However, we do not plan to use higher organic flow rate at this time.

In January, we plan to build a hollow fiber contained liquid membrane module needed for the alternative process for regenerating SO_2 scrubbing liquor. The module will have two sets of fibers. The first set of fibers are made of microporous hydrophobic polypropylene (Celgard X-10 hollow fibers). The second set of fibers are made of silicone rubber (Silastic tubing). We have already acquired the Celgard fibers from Hoechst Celanese Corp., Charlotte, NC. The Silastic tubings are being ordered from Baxter Healthcare Corp., Edison, NJ.

APPENDIX A

Consider the reaction:

$$A(g) + B(l) = C(l) \qquad \text{(A-1)}$$

where A is in the gas phase and B is a compound in the liquid phase that complexes with A to from C, also in the liquid phase. When A at concentration C_0 is fed to a bubbler containing B, the concentration of A leaving the bubbler will be reduced initially. As B becomes saturated with A, this exit concentration of A will increase with time. This concentration change of A over time is called the break through curve. A typical one was shown in Figure 2 for NO being absorbed by aqueous Fe(II)-EDTA. From such data, we can readily calculate the solubility of A in the liquid as well as the equilibrium constant K for the reaction listed in Eq. (A-1).

To obtain the solubility, we first write a mass balance:

amount of solute accumulated in liquid = amount of solute in - amount of solute out

$$= QC_0t_s - Q\int_0^{t_s} C\ dt \qquad \text{(A-2)}$$

where Q is the total gas flowrate, C_0 is the inlet concentration of A, and t_s is the time at which the outlet and inlet concentration of A are the same. Dividing by the liquid volume V yields:

$$C_s = \frac{QC_0}{V} t_s - \frac{Q}{V}\int_0^{t_s} C\ dt \qquad \text{(A-3)}$$

where C_s is the total solubility of A in the liquid. Thus the area between the break through curve and a horizontal line at C_0, i.e., the area above the break through curve, is proportional to the solubility as implied by Eq. (A-3).

From this data, we can also compute the equilibrium constant. First, however, we write the reaction in the form:

$$A(l) + B(l) = C(l) \qquad \text{(A-4)}$$

where A(l) is assumed to be in equilibrium with A(g). This equilibrium is often written as a Henry's law partition coefficient:

$$A(l) = H\,A(g) \tag{A-5}$$

Thus, we may write the equilibrium constant for the reaction listed in Eq. (A-4) as:

$$K = \frac{[C]}{[A(l)][B]} = \frac{[C]}{H[A(g)][B]} \tag{A-6}$$

By stiochemistry, we have

$$[C] = [B]_0 - [B] = C_s - [A(l)] \tag{A-7}$$

where $[B]_0$ is the concentration of B initially and C_s, given by Eq. (A-3). Thus we obtain:

$$K = \frac{C_s - H[A(g)]}{H[A(g)]\{[B_0] - C_s + H[A(g)]\}} \tag{A-8}$$

All quantities on the right side of this expression are now known, and we may readily calculate K.

DATE
FILMED
6/1/94
END